Tools for Teaching
GAS SEPARATION USING POLYMERS

David T. Coker, Rajeev Prabhakar*, Benny D. Freeman*
Research Triangle Institute • Research Triangle Park, NC 27709-2194

Gas separation with polymer membranes is rapidly becoming a mainstream separation technology. The most widely practiced separations are enriched nitrogen production from air, hydrogen separation in ammonia plants and refineries, removal of carbon dioxide from natural gas, removal of volatile organic compounds (*e.g.*, ethylene or propylene) from mixures with light gases (*e.g.*, nitrogen) in polyolefin purge gas purification, and water vapor removal from air.[1-3] Relative to conventional separation technologies, membranes are low-energy unit operations, since no phase change is required for separation. Additionally, membranes have a small footprint, making them ideal for use in applications on offshore platforms, aboard aircraft, and on refrigerated shipping containers, where space is at a premium or where portability is important. They have no moving parts, making them mechanically robust and increasing their suitability for use in remote locations where reliability is critical.[3]

Gas separation membranes are often packaged in hollow-fiber modules—a cartoon of such a module is presented in Figure 1. A full-scale industrial module for air separation may contain from 300,000 to 500,000 individual fibers in a tubular housing that is 6 to 12 inches in diameter and approximately 40 inches long. Each fiber will have inside and outside diameters on the order of 150 and 300 micrometers, respectively. For a typical case, the fiber wall, approximately 75 micrometers thick, consists of a very thin, dense separation membrane layer on the order of 500 to 1000 Å (0.05 to 0.1 micrometers) thick, on the outside of the fiber. This thin layer provides, ideally, all of the mass transfer resistance and separation ability of the hollow fiber. The remaining 74.9 to 74.95 micrometers of the fiber wall comprise a porous polymer layer that provides mechanical support for the thin membrane, but offers little or no mass transfer resistance. (To put fiber dimensions in perspective, the diameter of a typical human hair is about 100 micrometers.)

Gas (air in this example) flows under pressure into the module, where it is distributed to the bores of the fibers. In air separation, feed pressures of approximately 10 to 15 bar are typical. The air gases permeate through the wall of the fibers into the shell of the hollow-fiber module, which is maintained at essentially atmospheric pressure. The gas permeating through the fibers and into the shell is collected and leaves the module as the permeate stream.

Because oxygen, water, and carbon dioxide are more permeable than nitrogen and argon, the gas in the fiber bore is enriched in N_2 and Ar as it moves through the fiber lumens from the feed to the residue end of the module. This process can produce 99+% N_2 in the residue stream.

Such purified nitrogen is widely used for blanketing or inerting applications in, for example, the aviation (fuel tank blanketing), shipping (food container/packaging blanketing), and chemical industries (storage tank and line blanketing or

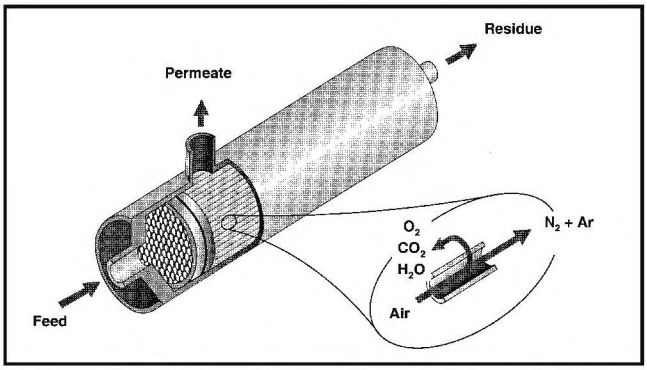

Figure 1. *Cartoon of hollow-fiber module used for air separation. From <www.medal.com> and Ref. 4.*

David T. Coker *provides engineering software services for Research Triangle Institute. He holds a BS in Chemical Engineering (1997) from North Carolina State University.*
Rajeev Prabhakar *is currently working toward his PhD in chemical engineering at the University of Texas at Austin. His research relates to the development of membrane-based systems for removal of carbon dioxide from natural gas streams. He received his BTech in chemical engineering from the Indian Institute of Technology (Kharagpur) and his MS from North Carolina State University.*
Benny D. Freeman *is the Matthew van Winkle Professor of Chemical Engineering at the University of Texas at Austin. His research is in polymers, particularly the sorption, diffusion, and permeation of small molecules through polymers and polymer-based composites.*

* *University of Texas at Austin, Austin, TX 78758*

purging)(see <www.medal.com> for further examples).

This paper presents a brief background section describing the fundamentals of gas transport in polymer membranes and then discusses models of mass transfer in gas separation modules. First, an analytical model for binary gas separation will be described, and it can be used to rapidly develop intuition regarding the effect of membrane process variables on separation performance. Then, a more rigorous model, which is available on the Internet, will be described—this model can be used to perform more realistic simulations and address more complex situations (*e.g.*, multicomponent separations, use of sweep streams to enhance separation efficiency, staging membrane units, recycle, etc.).

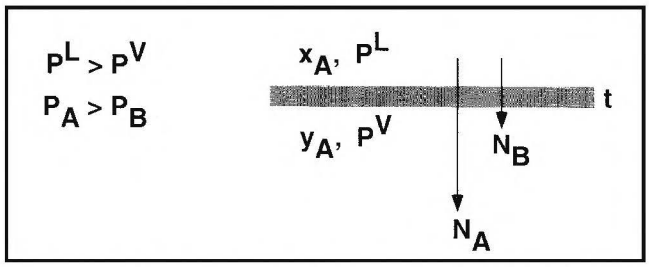

Figure 2. *Schematic of a gas separation membrane of thickness t being used to separate a gas mixture of components A and B (O_2 and N_2, for example). The upstream pressure, P^L is greater than the downstream pressure, P^V, and the mol fractions of component A on the upstream and downstream sides of the membrane are x_A and y_A, respectively. The steady state fluxes of components A and B through the membrane are N_A and N_B, respectively. By convention, component A is selected so that the permeability of the membrane to component A, P_A, is greater than the permeability of the membrane to component B, P_B.*

TABLE 1
Oxygen and Nitrogen Permeability in Selected Polymers*

Polymer	*Oxygen Permeability (Barrer)*	*Nitrogen Permeability (Barrer)*	*Oxygen/Nitrogen Selectivity*
Poly(1-trimethylsilyl-1-propyne)	7600	5400	1.6
Poly(dimethylsiloxane)	638	320	2
Poly(4-methyl-1-pentene)	30	7.1	4.2
Poly(phenylene oxide)	16.8	3.8	4.4
Ethyl cellulose	11.2	3.3	3.4
6FDA-DAF (polyimide)	7.9	1.3	6.2
Polysulfone	1.38	0.239	5.8
Polyaramid	3.1	0.46	6.8
Tetrabromo bis polycarbonate	1.4	0.18	7.8

**These data are from Baker.[3] The unit for gas permeability, the Barrer, is named after Professor Barrer, one of the pioneers in this area.[7]*
1 Barrer = 10^{-10} cm^2(STP)cm/(cm^2s cmHg). For permeability values, standard temperature and pressure (STP) are 0°C and 1 atm, respectively.

BACKGROUND

The fundamental mechanism for gas transport across a polymer membrane was described by Sir Thomas Graham more than a century ago.[5] (This classic article, along with a number of other seminal papers in membrane science, are reproduced in the 100th volume of the *Journal of Membrane Science.*[6]) This mechanism, known as the solution/diffusion model, postulates a three-step process for gas transport through a polymer: 1) dissolution of the gas into the high-pressure (or high chemical potential) upstream face of the polymer, 2) diffusion of the gas through the polymer, and 3) desorption from the low-pressure (*i.e.*, low chemical potential) downstream face of the polymer. Steps 1 and 3 are very fast relative to step 2, so diffusion through the polymer is the rate-limiting step in mass transport across a membrane.

Figure 2 depicts a dense polymer film (or membrane) of thickness t exposed to a binary mixture of gases A and B. The mole fraction of A on the upstream, or high pressure, side of the membrane is x_A, and the mole fraction of A on the downstream, or low pressure, side of the membrane is y_A. The upstream pressure, P^L, is greater than the downstream pressure, P^V. Because separation membranes are so thin (500-1000Å), the characteristic timescale for gas molecule diffusion through the membrane is very fast, and as a result, industrial gas separation membranes typically operate at steady state. The flux of A across the film, N_A, is[2]

$$N_A = \frac{P_A}{t}\left(x_A P^L - y_A P^V\right) \qquad (1)$$

where P_A is the permeability of the polymer to component A. The ratio of permeability to membrane thickness is called the permeance of the membrane to gas A, and this ratio can be viewed as a mass transfer coefficient that connects the flux (often expressed in cm^3[STP] of gas permeated through the membrane per cm^2 of membrane area per second) with the driving force for transport, which is the partial pressure difference between the upstream and downstream sides of the membrane. (Standard temperature and pressure for permeance are 0°C and 1 atm, respectively.) A similar expression can be written for component B as

$$N_B = \frac{P_B}{t}\left[(1 - x_A)P^L - (1 - y_A)P^V\right] \qquad (2)$$

For a given gas molecule, every polymer has a different permeability coefficient. Based on the data in Table 1, oxygen permeability, for example, varies by orders of magnitude from one polymer to another. Moreover, in a given polymer, the permeability coefficient will vary from

one gas to the next, and it is this property that allows the polymer to separate gas mixtures. The data in Table 1 indicate that oxygen is always more permeable than nitrogen in all polymers, and the ratio of O_2 to N_2 permeability, the selectivity, varies from 1.6 to 7.8 in the materials shown. Typically, as the permeability of a polymer to oxygen increases, its selectivity decreases, and vice versa.[8,9] In the most widely used gas separation membranes, permeability coefficients often decrease with increasing gas molecule size, so most gas separation membranes are more permeable to small molecules (*e.g.*, H_2) than to larger molecules (*e.g.*, CH_4). There are interesting exceptions to this general rule, and membranes based on such materials may become more commonplace in the near future.[10-12]

ANALYTICAL CROSSFLOW MODEL

The mole fraction of gas A on the permeate or downstream side of the membrane is given by the flux of component A through the membrane divided by the total gas flux through the membrane

$$y_A = \frac{N_A}{N_A + N_B} = \frac{\frac{P_A}{t}\left(x_A P^L - y_A P^V\right)}{\frac{P_A}{t}\left(x_A P^L - y_A P^V\right) + \frac{P_B}{t}\left[(1-x_A)P^L - (1-y_A)P^V\right]} \tag{3}$$

This expression can be reorganized as follows to permit a direct calculation of permeate purity:

$$y_A = \frac{\left[1+(\alpha-1)\left(\frac{1}{R}+x_A\right)\right]}{\frac{2}{R}(1-\alpha)}\left[\left(1+\frac{\frac{4}{R}(1-\alpha)\alpha x_A}{\left[1+(\alpha-1)\left(\frac{1}{R}+x_A\right)\right]^2}\right)^{1/2} - 1\right] \tag{4}$$

where the selectivity, α, is defined as the ratio of permeability coefficients ($\alpha = P_A/P_B$) and the pressure ratio, R, is defined as the ratio of feed to permeate pressure ($R = P^l/P^v$). Equation 4 can be used to determine the effect of feed composition, pressure ratio, and membrane selectivity on the mole fraction of gas produced by a membrane.

There are two limits of Eq. (4) that provide insight into the factors that govern the ultimate separation performance of membranes. It is easier to see these two limits if, instead of using Eq. (4) directly, we use the following equivalent reorganized form of Eq. (3):

$$\frac{y_A}{\alpha(1-y_A)} = \frac{Rx_A - y_A}{R(1-x_A) - (1-y_A)} \tag{5}$$

Figure 3 presents the permeate purity as a function of membrane selectivity, and the two limits of interest are shown. The first limit to be discussed is the pressure ratio limit. As membrane selectivity increases, the permeate mole fraction, y_A, will increase, but y_A can only increase up to the point that the partial pressure of component A on the upstream side ($x_A P^L$) of the membrane equals that on the downstream side ($y_A P^V$). At this point, the driving force for transport of A across the membrane is zero, the flux of component A goes to zero, and there can be no further increase in the mole fraction of component A in the permeate. Therefore, in the limit of very high selectivity (*i.e.*, as $\alpha \to \infty$ in Eq. 5 and, therefore, Eq 4), Eq. (5) reduces to

$$y_A = Rx_A \tag{6}$$

That is, at high selectivity, the purity of gas produced is limited by the pressure ratio. Of course, the value of y_A can never be greater than unity.

This limit has industrial significance in situations were selectivity is very high and process conditions dictate a small pressure ratio between permeate and feed streams. An example is the removal of hydrogen from mixtures with hydrocarbons in hydrotreaters in refineries.[3] The hydrocarbons in such a mixture would be methane and higher hydrocarbons, all of which are less permeable than methane in the membranes used for such separations. Typically, H_2 is hundreds of times more permeable than CH_4 and other components in such a mixture.[2] But typical upstream and downstream pressures would be 120 and 30 bar, respectively,[3] so the pressure ratio would only be 4. In such a case, having very high selectivity does not result in much

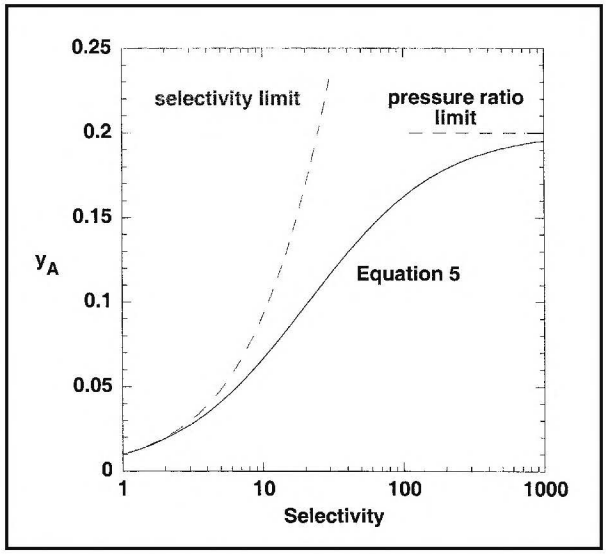

Figure 3. *Permeate purity as a function of membrane selectivity for a feed composition, x_A, of 1 mole percent A (99 mol percent B) and a pressure ratio of 20.*

higher-purity H_2 in the permeate because the H_2 permeation is at or near the limit where its partial pressure upstream and downstream are almost equal.

Another example is dehydration of gas streams such as air. Typically, water is much more permeable than air gases in polymers used for gas separation, so the amount of water that can be removed from a gas stream is often limited by the ability to keep the partial pressure of water very low in the permeate gas. This is often done by recycling some of the dry residue gas product back across the permeate side of the membrane to dilute the concentration of water being produced in the membrane. Such so-called purge or permeate sweep strategies can markedly reduce the dew point of air produced by dehydration membranes.[4]

At the other extreme, if the membrane is operated with a vacuum on the permeate side of the membrane (*i.e.*, $R \rightarrow \infty$), then Eq. 5 becomes

$$y_A = \frac{\alpha x_A}{1+(\alpha-1)x_A} \qquad (7)$$

and permeate purity is limited by polymer selectivity. As permeate pressure, P^V, decreases toward zero (or, equivalently, as the ratio of feed to permeate pressure increases to the point that the partial pressures of components A and B in the permeate become very small relative to their partial pressures in the feed), the flux of components A and B approach maximum values based on membrane permeability, thickness, composition, and upstream pressure

$$N_A \rightarrow \frac{P_A}{t} x_A P^L \quad \text{and} \quad N_B \rightarrow \frac{P_B}{t}(1-x_A)P^L \qquad (8)$$

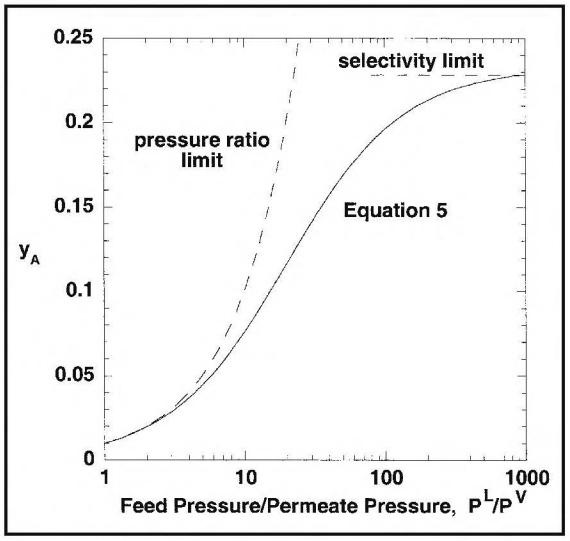

Figure 4. *Permeate purity as a function of pressure ratio for a feed composition, x_A, of 1 mole percent A (99 mol percent B) and a selectivity of 30.*

When the expressions in Eq. (8) are used to evaluate permeate purity based on $y_A = N_A/(N_A+N_B)$, Eq. (7) is obtained. In this case, the mole fraction of component A in the permeate is then limited by the ability of the membrane to prevent transport of component B across the membrane; that is to say, permeate purity is limited by membrane selectivity. This limit is shown in Figure 3 and also in Figure 4, which presents permeate mole fraction as a function of pressure ratio. This limit is reached when the pressure ratio is very high or the membrane selectivity is low.

An example of practical importance is the separation of N_2 from CH_4 in natural gas wells, a separation that is currently not practiced industrially using membranes because of this issue.[3] Many natural gas wells are contaminated with nitrogen, which would need to be removed to bring the heating value of the natural gas to pipeline specifications.[3] But polymer membranes rarely have an N_2/CH_4 selectivity greater than 2. In this case, even for large pressure ratios, the separation of this gas mixture is not good using membranes. For example, when the feed mole fraction of N_2 is 2%, the permeate mole fraction of N_2 is only 3.9%, and at a feed mole fraction of 20%, the permeate mole fraction is only 33%. There is little separation, and most of the low-pressure permeate waste gas is methane. That is (because the separation is poor), there is a large loss of methane into the low-pressure permeate stream with little removal of N_2 from the feed gas.

INTERNET MODEL

The analytical model described above is applicable to separation of binary mixtures only. Moreover, it does not account for the fact that as the feed gas travels through the hollow fibers, its composition changes as selective permeation strips the more permeable components from the feed-gas mixture. A classic extension of this model, due to Weller and Steiner, takes this factor into account.[13] This model, however, is no longer strictly an analytical solution, Moreover, it cannot simulate the countercurrent flow patterns that are used industrially in gas-separation modules. As indicated qualitatively in Figure 1, typical industrial permeators are designed to allow the feed gas and permeate gas to flow countercurrent to one another. Moreover, this model does not allow for separation of multicomponent mixtures of gases, which is a major practical limitation.

The simple model described above has been extended to account for multicomponent gas separation and to simulate countercurrent flow.[4,14] In this case, the governing mass balance equations are coupled differential equations, and no analytical solution is available. Numerical solutions to this model are available for public use at

http://membrane.ces.utexas.edu

The basic notion underlying the multicomponent, countercurrent simulator developed by Coker, *et al.*, is presented in Figure 5, which shows a diagram of the hollow-fiber module from Figure 1 divided axially into N slices or stages. In a typical simulation, N ranges from a few hundred to several thousand, depending on how rapidly the concentration of the most permeable species changes with axial position along the module. Inside each stage of the membrane, mass transfer occurs according to Eq. (1), which is written analogously for each component.

Using an approach originally developed for staged unit operations such as distillation,[15] the flow of each component from stage to stage is linked by a mass balance. The set of mass balances for each component on each stage can be written in the form of a family of tridiagonal matrices, which are solved using the Thomas algorithm.[16] The mass balances are nonlinear, so an iterative solution is required. Moreover, the model allows for pressure in the bore of the hollow fibers to change according to the Hagen-Poiseuille equation, and this introduces another source of nonlinearity into the problem. The details of the solution are provided in the literature.[4]

The simulation is organized to perform analysis calculations. That is, the membrane permeation characteristics, thickness, fiber inner and outer diameter, fiber length, and number of fibers are all specified via a graphical user interface, shown in Figure 6. The user may select bore-side or shell-side feed. It should be noted that the model is based on plug flow of gas through the module and fibers, so effects associated with gas maldistribution in the module are not captured. The reader is directed to the work of Lipscomb and colleagues for a more detailed description of these effects.[17]

The so-called "pot length" of the fibers must be specified in the simulation. When membrane fibers are assembled into a module, the membrane bundle is glued or "potted" on both ends in epoxy to provide a leak-free connection between the fiber bundle and the module housing. Gas can travel down the bore of the fibers in the potted region of the module, which leads to a pressure drop along the bore of the fibers, but because the fibers are covered with epoxy, there is no gas transport across the fiber wall. Typical values of pot length would be 10 cm on each end of a fiber 100 cm long. So, in the case, the "active" length of a fiber (*i.e.*, the length of fiber that is active for mass transfer via permeation) would be 100 cm - 2x10 cm (since the fiber is potted on both ends) = 80 cm.

An on-line databank is available with permeation properties of a few common polymers, such as polysulfone, or the users can supply their own permeation properties. The feed pressure, feed flowrate, feed composition, and permeate pressure are specified by the user. With these inputs, the simulator calculates the concentration, flow and pressure profiles in the module, the residue and permeate composition and flowrate, and the residue pressure. The concentration and flow profiles can be viewed as graphs built into the simulator. A user can establish an account where membrane fiber and module data are stored, so that simulation conditions can be entered and stored for later use. Several example simulations can be downloaded as pdf files.

USING THE INTERNET MODEL FOR TEACHING

Two examples of the use of the model are presented. Other examples are given in the literature.[4,14] The first case involves a membrane for air drying. The objective is to remove water from air and produce dry air as the residue stream. In conventional gas-separation membranes, water is typically more permeable (by a factor of 50 or more) than air gases such as N_2 and O_2, so H_2O/N_2 and H_2O/O_2 selectivities are very high. Additionally, the mol fraction of water in air is low. For example, air at 40°C and 10 atmospheres total pressure (conditions that are common for feeding a gas-separation module for air separations), the mole fraction of water at saturation is

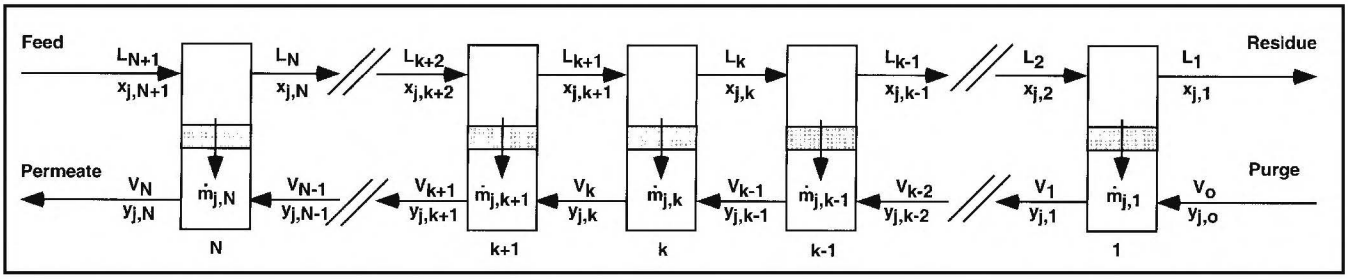

Figure 5. *Schematic of hollow-fiber module divided into N stages. In analogy with labeling conventions used in distillation, the flow rate of gas leaving the upstream (i.e., residue) side of stage k is labeled L_k, and the flow rate of gas leaving the downstream (i.e., permeate) side of stage k is labeled V_k. The flow rate of gas of component j that permeates from the upstream to the downstream side of stage k is $\dot{m}_{j,k}$. The mole fractions of component j leaving stage k on the upstream and downstream sides of the membrane are $x_{j,k}$ and $y_{j,k}$, respectively. Adapted from the literature.[4]*

0.72%.[18] These conditions (high selectivity, low feed concentration) lead to pressure-ratio-limited separation, and the amount of water removed from the gas stream is strongly dependent on the downstream partial pressure of water.

If one could lower the downstream partial pressure of water or otherwise accelerate the removal of water from the permeate side of the membrane, then the amount of water that could be removed from the air fed to the module would be enhanced. In practice, this is most often achieved by recycling a small fraction of the dry residue gas to the permeate side of the membrane, as illustrated in Figure 7. This has the benefit of sweeping or purging the permeate of components (*i.e.*, water) that have been preferentially removed by the membrane—this recycle stream is often called a purge or sweep stream.

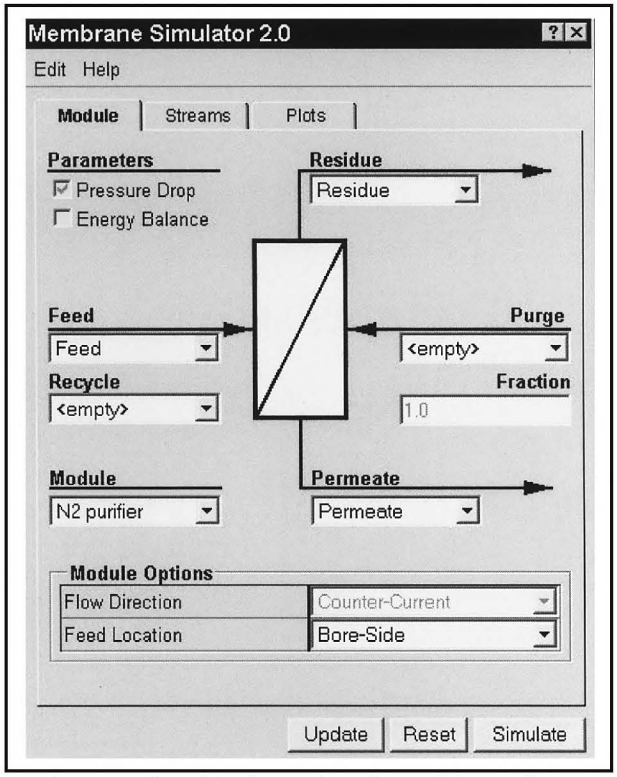

Figure 6. *Graphical user interface of the on-line membrane simulator at http://membrane.ces.utexas.edu*

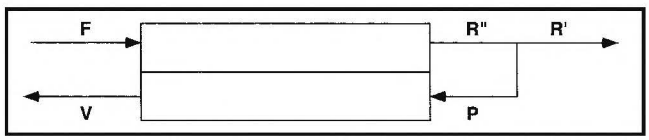

Figure 7. *Gas flow configuration in which a portion of the residue stream, P, is returned to the permeate side of the membrane as a sweep or purge stream to increase the driving force for removal of water. Adapted from Coker, et al.[4] The feed gas flow rate is F, the permeate flow rate is V, and the final residue flow rate of product gas is R'.*

An interesting calculation is to determine the effect of changes in the fraction of the residue stream that is recycled on the water concentration in the product residue gas, usually expressed as the dew point of the residue gas. The general trend, shown in Figure 8, is that using more gas to purge the permeate results in better water removal from the residue (*i.e.*, lower dew point). This results in a smaller amount of the dry product gas being available for use, however, so there is a trade-off between gas dryness and production rate.

Other problems that could be envisioned include replacing the polymer (which is polysulfone in the case of the results presented in Figure 8) with other polymers having different selectivities for water and determining the impact of separation factor on the fraction of residue purge gas needed to achieve a given dewpoint using a standard-size module. A good first approximation of the reduction in the amount of residue gas available for use is the flowrate of residue gas in the absence of purging times the fraction of residue gas removed for purging. This rule-of-thumb is not exact, how-

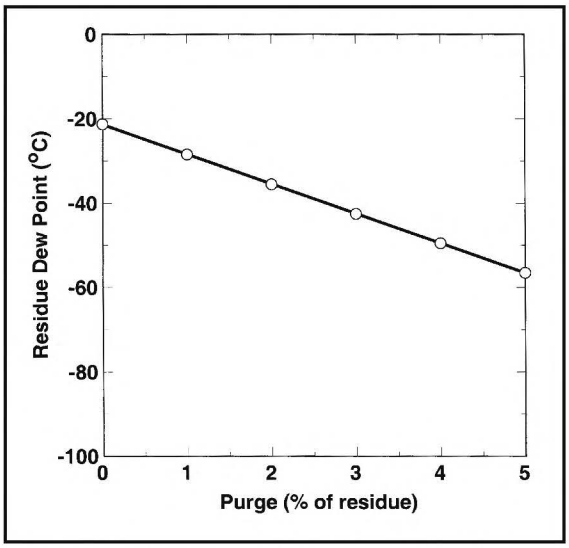

Figure 8. *The effect of permeate purge on the dew point of the residue gas obtained by feeding air to a module at 40°C and 10 atm. The permeate pressure is 1 atm, and the permeance of the membrane to water is 1,000x10^{-6} cm^3(STP)/(cm^2 s cmHg). Standard temperature and pressure for permeance, like permeability, are 0°C and 1 atm. The feed air flowrate is 8,000 ft^3(60°F, 1 atm)/hr. Specifying gas flowrates at 60°F and 1 atm (rather than at STP) is standard in some process simulators. Other parameters (number and length of fibers, permeance to all other components, etc.) are given in the literature.[4] The water mole fraction data in the residue stream were converted to dew points using a web-based psychometric calculator at http://www.connel.net/freeware/psychart.shtml*

ever, and it is of interest to allow students to figure out what other factors (*i.e.*, driving force for other components in the feed gas, etc.) might also influence the residue-gas flow rate for such problems.

The second example is hydrogen recovery from a hydrotreatment unit in a refinery. In hydrotreatment, petroleum intermediates are contacted with hydrogen to reduce sulfur, nitrogen, metals, asphaltene, and carbon residue content. This process requires substantial amounts of hydrogen gas, and much of the excess hydrogen can be recycled. Membranes are often used to purify the recycled hydrogen. The major impurities are light hydrocarbons. A typical stream might contain 65 mol % H_2, 21 mol % CH_4, and the balance will be other hydrocarbons, such as C_2 and C_3.[4]

In the conventional membranes used in this process, hydrogen is by far the most permeable component in the mixture, followed by methane and then by the other hydrocarbons. H_2/CH_4 selectivity values can be of the order of several hundred in commercially used membrane materials.

The objective of this separation is to generate highly purified hydrogen for recycle to the process. Because this is a high-pressure process and because the H_2 product appears in the permeate stream, permeate pressure must be kept as close to the feed pressure as possible to minimize recompression costs. So the pressure ratio is typically not very high. At fixed feed and permeate pressure, the more feed gas that is allowed to permeate through the membrane (by having lower flow rates or larger membrane area, or both), the higher is the recovery of hydrogen in the permeate, but the purity of the permeate stream is lower. So it is instructive to construct so-called purity/recovery curves for this separation.

One example is shown in Figure 9. The curves in this figure were generated by varying the feed flow rate to a module and noting the permeate H_2 purity and flowrate. That is, at very high flow rates, one can produce relatively pure H_2, but the amount of H_2 recovered in the permeate stream is very low. At the opposite extreme, at very low flow rates, most of the H_2 and CH_2 gas permeates through the membrane, so H_2 recovery is very high, but the purity is quite low. The ideal situation would be to have both high recovery and high purity, but these factors typically work against one another.

Figure 9 also illustrates the impact of pressure ratio on the results. Two pressure scenarios are presented. In both cases, the difference between feed and permeate pressure is identical. The case with lower feed pressure and higher pressure ratio yields superior membrane separation performance, however. Such sensitivity of purity/recovery curves is an indication that the separation is being performed in a pressure-ratio-limited regime.

Other interesting problems include calculating purity/recovery curves for other polymers to understand how the choice of polymer material influences the separation. In this regard, there is a large database of permeability values in the *Polymer Handbook.*[19] Also, the hydrotreater example as well as the air separation example involve multicomponent mixtures, and one could track the distribution of each of the other components as polymer selectivity, flowrate, feed, or permeate pressure changes. We have used the analytical simulator as well as the Internet version of the simulator in the senior-level design course, and it should be suitable for an undergraduate unit operations course as well.

The Internet simulator allows exploration of the effects of operating the module with bore-side feed or shell-side feed. It is of interest to compare the same separation (*e.g.*, air separation) using bore- and shell-side feed and to explain differences in the separation results. Basically, when the membrane module is fed on the bore side, the permeate gas is collected on the shell side of the module and experiences essentially no pressure drop traveling from one end of the module to the other. There is a slight decrease in pressure along the bore of the fibers, but this decrease is typically small relative to the feed pressure and has a small impact on separation performance.

With shell-side feed, however, the permeate gas flows in the bore of the fibers, and pressures are much lower in the permeate stream than in the residue stream. Small pressure changes along the bore of the fibers, estimated according to the Hagen-Poisseulle relation, can lead to decreases in sepa-

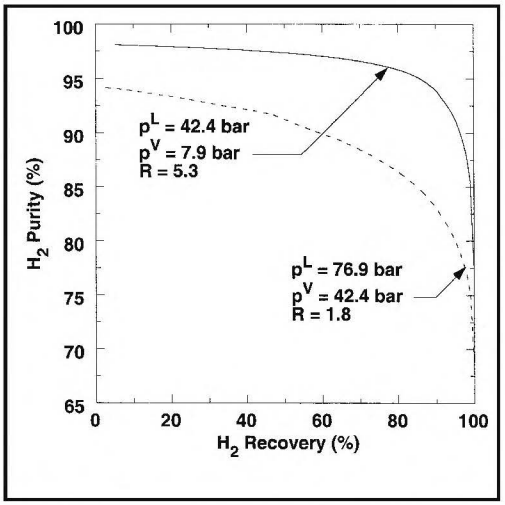

Figure 9. *Effect of pressure ratio on H_2 purity and recovery in a hydrotreater application. The membrane properties and module conditions as well as the feed composition are given in Coker, et al.*[4] *H_2 recovery in the permeate is the molar flowrate of hydrogen in the permeate divided by the molar flowrate of hydrogen fed to the module.*

ration efficiency (lower product purity, less gas permeated per unit area of membrane) relative to bore-side feed.

Additionally, the Internet simulator allows connection of the outlet stream (*e.g.*, residue) from one module as the feed stream to a second module. This feature allows exploration of the effect of connecting modules in series on product gas purity and flowrate. Similarly, the Internet simulator is organized to allow the product gas from one module to be recycled to the feed side of a previous module. Downloadable example files illustrate the use of these features.

If students have access to process simulation tools, comparison with other separation technologies can be interesting. For example, large-scale air separation is currently performed using cryogenic distillation. If one requires only 98% nitrogen for an application (rather than pure nitrogen), current membranes with an O_2/N_2 selectivity of 7 or 8 can readily produce gas at this purity level.

An interesting calculation is to compare capital and operating costs for a cryogenic air-separation plant and a membrane-separation plant to produce nitrogen at such purities. Some variables that could be studied include required product gas flowrate, purity, and pressure. For such rough economic analyses, the installed costs of membranes have been estimated as \$54/m^2 of membrane surface area.[20] For a membrane process, the process operating cost is the energy input required to compress air from one atmosphere to the 10-15 atmosphere range normally used for air-separation membranes. Therefore, the higher the purity of the product required, the lower the product recovery and the greater the energy waste due to loss of nitrogen into the low-pressure permeate stream.

Currently, membrane processes do not scale as well as conventional separation technologies. That is, to double the amount of gas being processed by a membrane plant, one needs to install twice as much membrane area, so the capital cost scales linearly with gas flowrate. Processes depending on column-based technology, such as distillation, exhibit much slower increases in capital costs with increasing flow rate, and this factor has led to membranes being used for lower flowrate applications and distillation being used for high-flowrate situations.[2] One could also explore the effect of new membrane materials development on such a separation. If the O_2/N_2 selectivity of today's membranes could be raised from 7 to 14, how would this influence the capital and operating costs associated with nitrogen production?

CONCLUSION

We have described some basic issues related to the use of polymeric membranes as separation agents, and we have provided two types of tools—one analytical and one Internet-based—to assist students in gaining intuition into the performance of gas separation membranes. Examples provide some basis for homework or class project activities. Some extensions to the problems discussed in this manuscript would have a significant design component, which might increase their utility.

REFERENCES

1. Zolandz, R.R., and G.K. Fleming, "Gas Permeation" in *Membrane Handbook,* W.S.W. Ho and K.K. Sirkar, eds, Van Nostrand Reinhold, New York, NY, p. 17 (1992)
2. Ghosal, K., and B.D. Freeman, "Gas Separation Using Polymer Membranes: An Overview," *Polym. Adv. Tech.,* **5**(11), 673 (1994)
3. Baker, R.W., *Membrane Technology and Applications,* McGraw-Hill Book Co., New York, NY (2000)
4. Coker, D.T., B.D. Freeman, and G.K. Fleming, "Modeling Multicomponent Gas Separation Using Hollow-Fiber Membrane Contactors," *AIChE J.,* **44**(6), 1289 (1998)
5. Graham. T., "On the Absorption and Dialytic Separation of Gases by Colloid Septa. Part I. Action of a Septum of Caoutchouc," *Phil. Mag.,* **32** 401 (1866)
6. Graham, T., "On the Absorption and Dialytic Separation of Gases by Colloid Septa. Part I. Action of a Septum of Caoutchouc," *J. Membrane Sci.,* **100,** 27 (1995)
7. Michaels, A.S., "A Sixty-Year Love Affair with Membranes: Recollections of Richard M. Barrer, Edited and Annotated by Alan S. Michaels," *J. Membrane Sci.,* **109**(1), 1 (1996)
8. Robeson, L.M., "Correlation of Separation Factor Versus Permeability for Polymeric Membranes, *J. Membrane Sci.,* **62**, 165 (1991)
9. Freeman, B.D., "Basis of Permeability/Selectivity Tradeoff Relations in Polymeric Gas Separation Membranes," *Macromolecules,* **32**, 375 (1999)
10. Baker, R.W., and J.G. Wijmans, "Membrane Separation of Organic Vapors from Gas Streams," in *Polymeric Gas Separation Membranes,* D.R. Paul and Y.P. Yampol'skii, eds., CRC Press, Boca Raton, FL (1994)
11. Freeman, B.D., and I. Pinnau, "Separation of Gases Usoing Solubility-Selective Polymers," *Trends in Poly. Sci.,* **5**(5), 167 (1997)
12. Freeman, B.D., and I. Pinnau, "Polymeric Materials for Gas Separations," in *Polymeric Membranes for Gas and Vapor Separations: Chemistry and Materials Science, ACS Symposium Series Number 733,* B.D. Freeman and I. Pinnau, eds., American Chemical Society, Washington, DC (1999)
13. Weller, S., and W.A. Steiner, "Fractional Permeation Through Membranes," *Chem. Eng. Prog.,* **46**(11), 585 (1950)
14. Coker, D.T., T. Allen, B.D. Freeman, and G.K. Fleming, "Nonisothermal Model for Gas Separation Hollow-Fiber Membranes," *AIChE J.,* **45**(7), 1451 (1999)
15. Stichlmair, J., and J.R. Fair, *Distillation: Principles and Practices,* John Wiley & Sons, New York, NY (1998)
16. King, C.J., *Separation Processes,* McGraw-Hill, New York, NY (1980)
17. Lemanski, J., and G.G. Lipscomb, "Effect of Shell-Side Flows on Hollow-Fiber Membrane Device Performance," *AIChE J.,* **41**(10), 2322 (1995)
18. Felder, R.M., and R.W. Rousseau, *Elementary Principles of Chemical Processes,* John Wiley & Sons, New York, NY (1986)
19. Pauly, S., "Permeability and Diffusion Data," in *Polymer Handbook,* 4th ed., J. Brandrup, E.H. Immergut, and E.A. Grulke, eds., John Wiley and Sons, New York, NY (1999)
20. Baker, R.W., "Future Directions of Membrane Gas Separation Technology," *Ind. Eng. Chem. Res.,* **41**, 1393 (2002) ❐